ICHS 2019: 8th International Conference on Hydrogen Safety
Adelaide, Australia, September 24-26, 2019

HYDROGEN DEFLAGRATIONS IN STRATIFIED FLAT LAYERS IN THE LARGE-SCALE VENTED COMBUSTION TEST FACILITY

Liang, Z., Gardner, L., Clouthier, T., MacCoy, R.
Canadian Nuclear Laboratories, Chalk River, Ontario, Canada
***Corresponding author*: zhe.liang@cnl.ca**

ABSTRACT

This paper examines the flame dynamics of vented deflagration in stratified hydrogen layers. It also compares the measured combustion pressure transients with 3D GOTHIC simulations to assess GOTHIC's capability in simulating the associated phenomena. The experiments were performed in the Large-Scale Vented Combustion Test Facility at the Canadian Nuclear Laboratories. The stratified layer was formed by injecting hydrogen at a high elevation at a constant flow rate. The dominant parameters for vented deflagrations in stratified layers were investigated. The experimental results show that significant overpressures are generated in stratified hydrogen–air mixtures with local high concentration although the volume-averaged hydrogen concentration is non-flammable. The GOTHIC predictions capture the overall pressure dynamics of combustion very well, but the peak overpressures are consistently over-predicted, particularly with higher maximum hydrogen concentrations. The measured combustion overpressures are also compared with Molkov's model prediction based on a layer-averaged hydrogen concentration.

1.0 INTRODUCTION

During postulated severe accidents with core degradation in nuclear power reactors, a large amount of hydrogen can be produced. If the hydrogen is uniformly dispersed throughout the containment building, the average hydrogen concentration may not be a safety concern [1]. However, the hydrogen may temporarily exist in non-uniform or stratified mixtures, possibly during the transient period before complete mixing has been achieved, or in regions where steam is continually condensing. Stratification of hydrogen is a safety concern because pockets of high hydrogen concentration may lead to a fast deflagration or detonation, which would challenge the integrity of the containment building. Combustion behaviour of uniform mixtures has been extensively either studied or reported in the literature using tube-like geometries (horizontal or vertical cylinders), but the reactor compartments have irregular shapes and the mixture in post-accident containments may be stratified. Questions have been raised regarding the validity of traditional safety criteria (that is, deflagration-to-detonation transition or DDT limits) developed from experiments performed with uniform mixtures in simple geometries. Although the DDT limits in stratified mixtures are not well established yet, significant progress has been made by many researchers.

Flame propagation in a vertical direction through stratified hydrogen mixtures in closed large-scale cylinders was examined by Whitehouse et al. [2] and Bleyer et al. [3]. They showed that the flame can be accelerated to a higher velocity in stratified mixtures than in well-mixed mixtures for the same overall hydrogen content when ignited from the higher hydrogen concentration region. Flame propagation in a horizontal direction through vertically stratified hydrogen mixtures was studied in rectangular channels with large aspect ratio by Vollmer et al. [4], Kuznetsov et al. [5], Rudy et al. [6], and Grune et al. [7]. Vollmer et al. [4] demonstrated that the DDT limit shifted to either considerably higher or lower fuel concentration depending on the obstruction configuration, such that the conventional "7λ" DDT criterion is no longer valid for stratified mixtures. Critical conditions for the onset of detonation in stratified mixtures in partially-confined flat layers contained in a closed 100 m^3 vessel were extensively examined by German researchers at the Karlsruhe Institute of Technology (KIT) and at Pro-Science Gmbh [5]–[7], but combustion characteristics of stratified hydrogen air mixtures in a vented vessel are not well known.

Reactor containment buildings consist of many interconnected compartments. Combustion-generated overpressures in a post-accident containment building can be relieved by venting to adjacent compartments through relief panels or existing openings. As a result, studies on vented combustion behaviour have been extensively performed in the past three decades at the Canadian Nuclear Laboratories (CNL) (for example by Liang [8] [9]). Venting is also a common industrial practice to reduce the consequences of confined explosions in equipment and buildings. The use of hydrogen as a fuel has also motivated a great effort in vented hydrogen combustion studies (for example Carcassi and Fineschi [10] and Chao et al. [11]) and development of predictive methods (for example Molkov and Bragin [12]).

To address the concern with combustion characteristics of stratified hydrogen in a vented vessel, a series of experiments was conducted in CNL's Large-Scale Vented Combustion Test Facility (LSVCTF). Liang et al. [13] investigated stratified hydrogen combustion in one or two chambers and the flame interaction between the two chambers. The experimental results showed that the combustion overpressure was significantly higher when the hydrogen was concentrated in a thin layer rather than well mixed in the volume for a given amount of hydrogen mass.

This paper compares GOTHIC 8.2 simulations with the experimental results for a selected number of stratified combustion experiments performed in the half volume of the LSVCTF. GOTHIC [14] is a general purpose thermal-hydraulic code that has been used by the nuclear industry for containment analysis. The comparison will assess the capability of GOTHIC's built-in mechanistic combustion model. The paper also compares the measured combustion overpressures with predictions using Molkov and Bragin's model [12].

2.0 EXPERIMENTAL METHODS

2.1 Facility

The LSVCTF is a 120 m^3 (10 m long, 4 m wide, and 3 m high) rectangular structural steel test chamber enclosed in an insulated Quonset building. The test chamber is constructed of 1.25 cm thick steel plates welded to a rigid steel I-beam framework. The entire structure is anchored to a 1 m thick concrete pad. The end walls are covered with rectangular steel panels bolted to the end-wall structure. Removing the appropriate number of panels from the end wall can change the vent area to the outside. Internal walls, made of structural steel beams, can be inserted into the facility to divide the entire chamber into two or three volumes. Eight hydraulic fans are installed in a diagonal pattern on the side walls to mix the gases uniformly during gas addition or to generate turbulence during a test.

Fig. 1 depicts the test configuration used in this study. The tests presented in this paper were performed in the front chamber (57 m^3) of the LSVCTF by blocking off the vents on the central wall. The front wall had a 1.1 m^2 vent (two sections separated by a 20 cm thick central beam). Prior to the hydrogen addition, the vents were covered with aluminium foil that ruptured at low pressures (<1 kPa) during combustion. Ignition was achieved with a hermetically sealed 120 V TAYCO glow plug igniter. The igniter was located in the centre of the front chamber at a height of 2.5 m.

2.2 Measurements

The initial gas composition was analysed by a process mass spectrometer and sampled at 20 s intervals prior to the ignition. The mass spectrometer was calibrated using primary calibration gases of 10 to 30% H_2 by volume in nitrogen. (The gas concentrations are always expressed on a volume basis in this paper.) The uncertainty was within ±0.5% (absolute).

The flame front position was monitored by 26 fine-wire (0.075 mm diameter) exposed-junction type S thermocouples installed at a height of 2.5 m in the front chamber to monitor the flame front position. They were 0.5 m apart between the centre and front walls and 1 m apart between the two side walls.

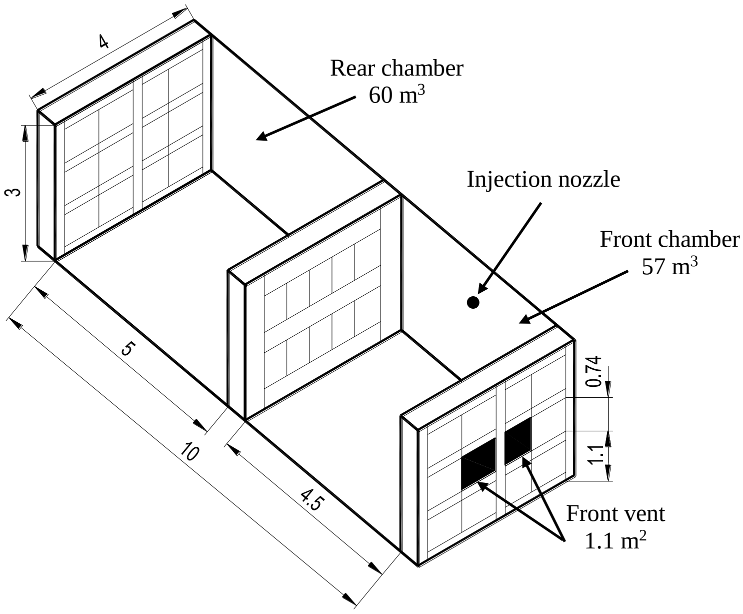

Figure 1. Schematic of large-scale vented combustion test facility

The transient pressure during combustion was monitored using six Kulite dynamic pressure transducers. The transducers were periodically calibrated with an Ectron pressure calibrator with an overall uncertainty of ~±0.5 kPa.

An infrared camera (Xenics Gobi-384 DCL50) was used to visualize the combustion events. It was calibrated for a temperature range of 300 to 1,200°C, but was able to discriminate temperature differences below 300°C with a resolution of ~1°C.

2.3 Test Conditions

A hydrogen injection nozzle was located on the side wall at a height of 2.5 m in the front chamber (Fig. 1). The hydrogen was injected normal to the side wall at a rate of ~6.7 g/min and a nozzle exit velocity of ~2.7 m/s, which corresponds to an injection Richardson number, *Ri*, of 0.07. As per Cariteau and Tkatschenko [15], the exit flow is usually jet-like (momentum-dominant) when $Ri \ll 1$, but it becomes plume-like (buoyancy-dominant) after a short distance from the nozzle, that is, after 0.14 m according to the correlation in Denisenko et al. [16]. Therefore, buoyancy would dominate the hydrogen dispersion in the current tests.

The LSVCTF was designed to maintain atmospheric pressure during the gas addition by venting gas through a 15 cm (6 in) diameter hole near the floor of the chamber. The vent was closed after the gas addition. Only air was expected to be vented out during the hydrogen injection because hydrogen would accumulate at the ceiling. During the hydrogen injection, the hydrogen concentration was continuously measured at seven locations on the wall opposite the injection, between the heights of 2.1 and 2.9 m. When the hydrogen concentration at a height of 2.9 m reached a desired value, the igniter was turned on to initiate combustion.

Fig. 2 shows an example of the hydrogen distribution along the height at selected injection times. Time zero corresponds to the start of hydrogen injection. The hydrogen concentration starts increasing immediately at the ceiling and the hydrogen accumulates above a height of 2 m during the entire gas injection. During the injection, the hydrogen plume clearly rises up along the side wall first, then spreads across the ceiling and fills the upper region, and then slowly moves downwards. The maximum hydrogen concentration at the ceiling and the layer thickness increase with the duration of the injection. The hydrogen concentration decreases nearly linearly from a height of 2.9 m to 2.5 m, but drops to near-zero from a height of 2.5 m to 2.1 m. The average slope of the hydrogen concentration decay is ~-0.29%

per cm between a height of 2.9 m and 2.5 m. The maximum hydrogen concentration is the measured value at a height of 2.9 m. The stratified hydrogen profile observed in the present study is similar to the results presented by Cariteau and Tkatschenko [15]. In their study, helium was injected from the floor in a sealed enclosure at a low flow rate (≤5 NL/min). The dispersion was dominated by buoyancy and the mixing behaviour followed a stratified regime in which the vertical helium distribution did not include a significant homogenous layer at the ceiling (that is, the thickness was less than 10% of the enclosure height).

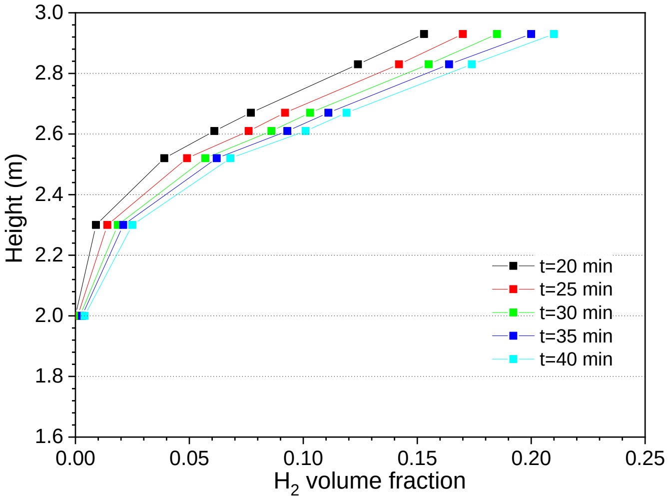

Figure 2. Vertical distribution of hydrogen in front chamber of LSVCTF with pure hydrogen injected at height of 2.5 m from side wall and with mass flow rate of 6.7 g/min

2.4 Test Matrix

The test conditions and key measurements of eight experiments are listed in Table 1. All the tests were performed under ambient conditions (1 atm, ~20–30°C, and ~50% relative humidity or RH). To simplify the data analysis, the hydrogen concentration was assumed to decrease linearly at a constant rate of 0.29% per cm from the maximum value at the ceiling to zero. The layer thickness is the distance between the point of zero hydrogen concentration and the ceiling. If the hydrogen in all these tests were well mixed in the front chamber, the mixture would not be flammable as the volume-averaged hydrogen concentration was less than 4.0% (which is the lower flammability limit).

Table 1. Summary of experimental conditions

Test ID	**P_0 (kPa)**	**T_0 (°C)**	**H_2 at 2.5 m (%)**	**H_2 at 2.9 m (%)**	**Layer Thickness (cm)**	**Avg. H_2 in Layer (%)**	**Avg. H_2 in 57 m^3 (%)**	**Pressure (kPa)**
SLS01	98.2	22.3	5.0	16.0	62.2	9.0	1.87	2.5
SLS02	98.2	23.0	4.5	17.4	67.0	9.7	2.17	3.5
SLS04	98.4	25.9	6.0	19.5	74.2	10.8	2.66	5.5
SLS09	98.7	22.7	6.8	21.1	79.8	11.6	3.07	9.1
SLS05	98.4	28.3	8.2	21.7	81.8	11.9	3.24	10.4
SLS10	98.7	23.4	8.3	22.6	84.9	12.3	3.49	12.1
SLS08	98.8	23.8	8.2	23.5	88.0	12.8	3.75	15.1
SLS07	98.7	22.5	10.7	24.3	90.8	13.2	3.98	20.3

3.0 NUMERICAL METHODS

3.1 GOTHIC Model

The GOTHIC model layout and its nodalisation are shown in Fig. 3. Control volume 1 represents the front chamber and is subdivided with a three-dimensional Cartesian mesh. The front chamber has nominal dimensions of 4.75 m long, 4.0 m wide, and 3.0 m tall. The length (X-direction) is subdivided with 15 uniform cells ($\Delta X = 0.317$ m). The width (Y-direction) is subdivided with 11 cells (10 cells with $\Delta Y = 0.38$ m and one with $\Delta Y = 0.203$ m at the midpoint). The height (Z-direction) is subdivided with 22 cells ($\Delta Z = 0.10$–0.23 m). The outside atmosphere, where the gas is expelled, is represented by control volume 2 (10 m tall; 4000 m^3 in volume). This volume is coarsely subdivided except for the region adjacent to the vent (~$2 \times 2 \times 2$ m^3 volume).

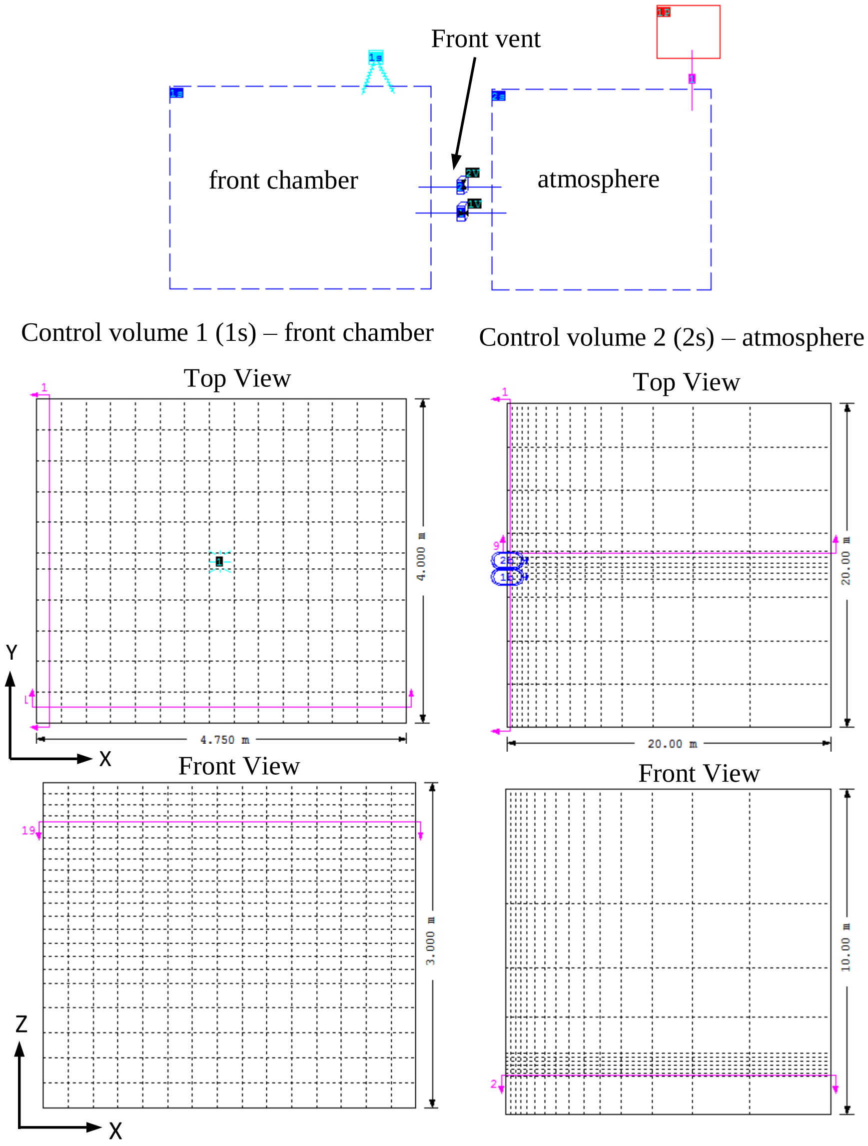

Figure 3. Schematic of GOTHIC model layout and subdivided volumes for LSVCTF

The 1.1 m^2 front vent was modelled using GOTHIC's built-in flow connectors, through which the adjacent cells in control volumes 1 and 2 were hydraulically connected. A quick-open valve was applied to the connectors with a user-defined OPEN trip to control the vent opening. The vent rupture pressure was set at 102 kPa. Sensitivity studies showed that a vent rupture pressure of 101 or 102 kPa had no influence on maximum peak pressures. A pressure boundary condition was applied to control volume 2 to maintain it at atmospheric pressure

Heat transfer between the fluid and the vessel ceiling was simulated. All conduction was modelled as one-dimensional and perpendicular to the structure surface. The inside surface of the ceiling was assumed to have a heat transfer coefficient of 200 $W/m^2 \cdot K$ and the outside surface was assumed to have a heat transfer coefficient of 0 (perfectly insulated). The heat loss to other walls was neglected because the burnt gas is mostly in contact with the ceiling. The default GOTHIC modelling options were used for mass and heat transfer (including condensation) and the standard two-equation κ-ε model was used to model turbulence.

3.2 Combustion Model

GOTHIC's mechanistic burn model was used to simulate combustion. When the mechanistic burn model is specified in a control volume and the mixture compositions satisfy the user-defined flammability limits, combustion of hydrogen is continuously calculated. The combustion rate is determined from the maximum of the laminar and turbulent burning rates. The former is defined as a function of laminar burning velocity and the latter is calculated using the wrinkled laminar flame model, which assumes the increase in burning rate due to turbulence is proportional to the amount of wrinkle along the reaction front. The amount of wrinkle is assumed to be proportional to the root-mean-square of the velocity fluctuation in the flow field.

Ignition of hydrogen is achieved by activation of an igniter component that is switched on at the beginning of the simulation and turned off after 0.1 s by an OFF trip. It provides a high effective temperature to initiate a high rate of chemical reactions inside the ignition cell. A burn enhancement factor of 2 was applied to the ignition cell in the current predictions to ensure a successful ignition due to the extremely lean mixture at the bottom of the stratified layer where the igniter is located.

3.3 Initial Conditions

An idealized initial condition (25°C, 100 kPa, 50% RH) was applied for all the simulations. As discussed in Section 2.4, the hydrogen concentration was set to decrease linearly from the maximum value (at the ceiling) to zero at a rate of 0.29% H_2/cm. The maximum hydrogen concentration was varied from a nominal value of 16% to a value of 26% in increments of 1% H_2 in each simulation.

4.0 RESULTS AND DISCUSSIONS

4.1 Pressure Transient

Fig. 4 shows a comparison of the time history of measured pressure for Test SLS07 with the GOTHIC simulation for a maximum of 24% H_2. The measured pressure trace was smoothed using a 50 Hz low-pass filter, and the maximum peak overpressures shown in Table 1 were also determined based on the smoothed curves. For easier comparison, time zero is aligned with the instance when the pressure increases by 0.01 kPa. The labels 1 to 6 are reference times to be used for discussions in Section 4.2.

Liang [8] showed that pressure transients of LSVCTF tests always exhibit multiple pressure peaks controlled by various mechanisms under initially quiescent conditions. The maximum peak overpressure of all quiescent tests are dominated by the acoustic coupled effect for hydrogen concentration greater than 8%, but the acoustic effect becomes insignificant under turbulent conditions. Fig. 4 shows that the pressure structure of combustion in a stratified layer is similar to that of well-mixed turbulent combustion, where there is one dominant peak corresponding to the instance when the flame reaches its maximum surface area (that is, when it encounters the vessel wall). A peak caused by a vent rupture is not visible, because the gas expansion (reaction rate) is sufficiently fast to overcome the gas loss through venting. After the maximum peak, a low-frequency and low-amplitude oscillation appears in the pressure signal because the bulk gas is disturbed and moving back and forth through the vent.

The simulation captures the overall pressure dynamics very well, and the calculated pressure increase before reaching the peak agrees well with the measurement, indicating that the flame speed is predicted well; however, the time to reach the maximum pressure and the maximum peak overpressure are slightly over-predicted. The over-prediction can be partially attributed to the difference in the hydrogen concentration distribution between the simulation and experiment. In the simulation, the hydrogen is assumed to be decreasing linearly from the ceiling, but the actual hydrogen concentration profile is not exactly linear. In the simulation, the hydrogen concentration is step-changed along the height and, therefore, the accuracy is limited by the grid size. The exact hydrogen profile is difficult to determine in the experiment due to the limited number of gas samples and unsteadiness of the hydrogen injection rate.

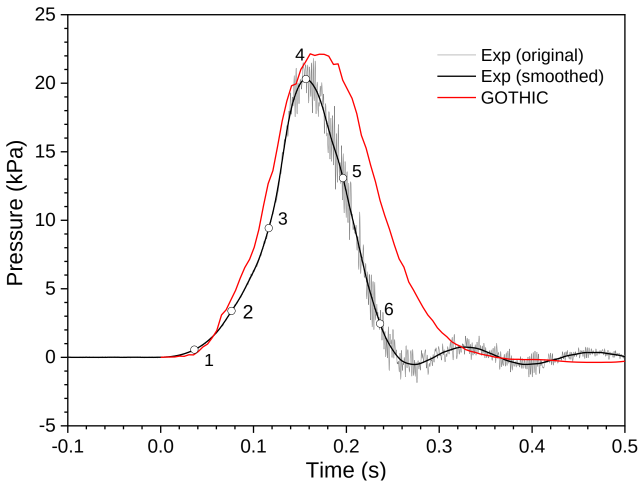

Figure 4. Comparison of GOTHIC simulations with measured combustion pressure transient for Test SLS07 (maximum 24% H_2 at ceiling)

Fig. 5 compares the calculated pressure transients with the measurements for a maximum hydrogen concentration of 17 to 23%. The general features are the same as those of the test shown in Fig. 4. With a higher maximum hydrogen concentration, the pressure increases sharply due to faster flame expansion. The pressure increase slows down slightly at the instance of vent rupture, but the effect is much less significant for the tests with higher hydrogen concentrations. The slope change also occurs at a much higher pressure than the vent rupture pressure (~1 kPa) due to the fast reaction rate of these mixtures. With a lower hydrogen concentration, the pressure stops increasing for a short time period after the vent rupture, resulting in a much longer time to reach the second peak. The overall pressure dynamics are well captured in the GOTHIC simulations. Similar to the test shown in Fig. 3, the calculated pressure transients for these tests match well with the measurements before the maximum pressures are reached, but the maximum overpressures are all over-predicted for the maximum hydrogen concentration greater than 17%.

4.2 Flame Dynamics

The burning process of Test SLS07 is demonstrated with infrared images in Fig. 6. The camera was located on the floor of the front chamber close to the centre wall facing the front wall. The corresponding time for each image is labelled on the pressure curve in Fig. 5. After the ignition at 0.036 s, a hot pocket is visible close to the igniter (1^{st} image). The fireball expands radially and the flame propagation is symmetric in all directions. The flame front is stretched towards the vent in the 2^{nd} image, indicating that the front vents have ruptured before 0.076 s and "cold" gas has started to exit from the front chamber to the atmosphere. As the bottom of the stratified layer is above the top edge of the front vents, the "cold" gas is expected to consist of only air. Hot gas venting is visible in the 3^{rd} image, suggesting that the flame front has arrived at the front wall before 0.116 s. When the maximum overpressure is reached at about 0.156 s in Fig. 5, the burnt gas also reaches its maximum (>1000°C) as shown in the 4^{th} image, suggesting that the combustion has reached its maximum heat release. The gas temperature starts to decrease in the 5th and 6th images, meaning that combustion is completed and the front chamber has cooled down due to gas exchange with the atmosphere.

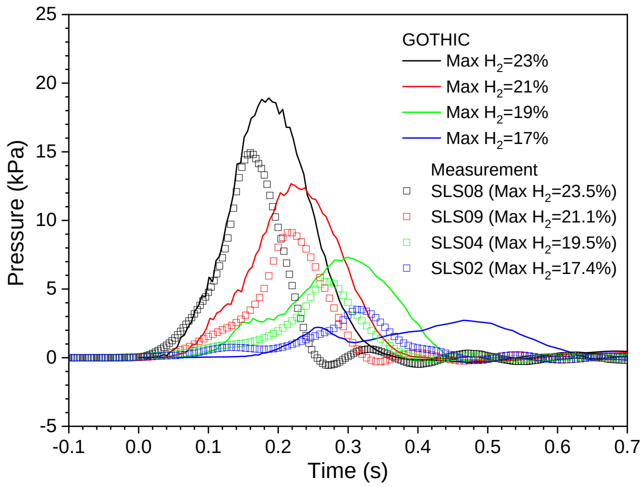

Figure 5. Comparison of GOTHIC simulations with measured combustion pressure for maximum 17-23% H_2 with -0.29%/cm gradient

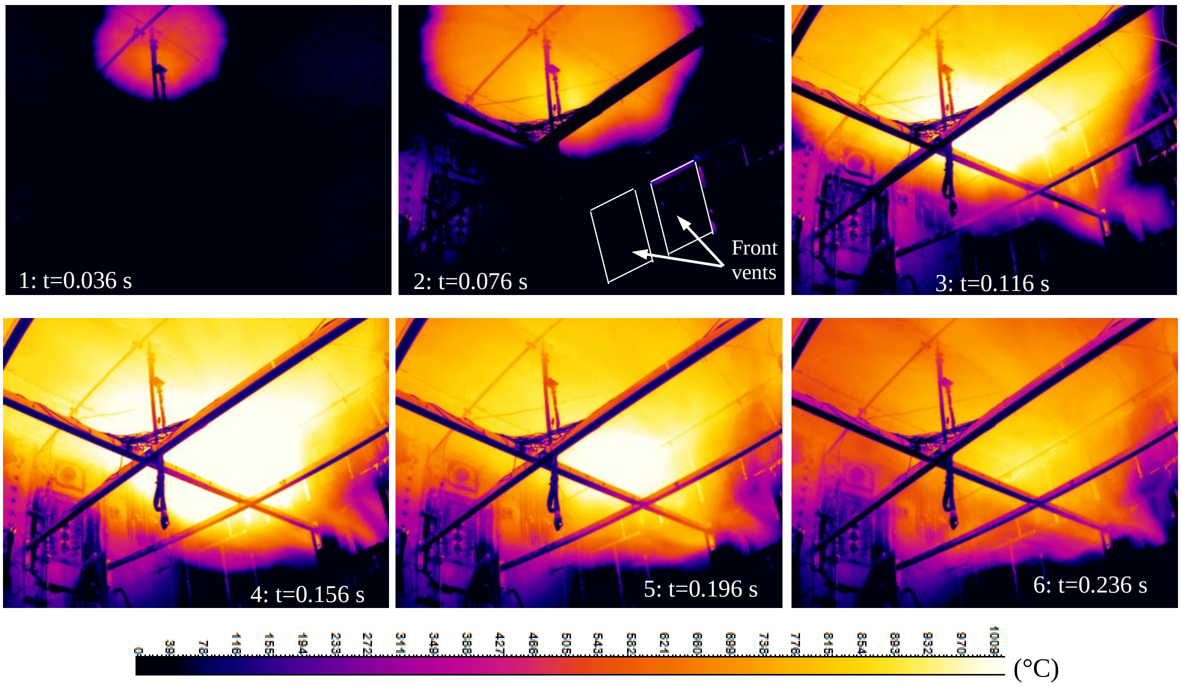

Figure 6. Infrared images of combustion for Test SLS07 (max 24.3% H_2)

Fig. 7 shows the two-dimensional contour plots of the GOTHIC simulation for gas temperature inside and outside of the front chamber (side view) between 0 and 0.22 s for a maximum of 24% H_2. The location of the vents is indicated as a rectangular box on each view. The initial hydrogen is concentrated above a height of 2.3 m. After the ignition starts in the centre, the flame ball expands symmetrically across the ceiling. The flame front arrives at the front wall at about 0.12 s, slightly faster than towards the back wall. Burnt gas starts flowing out from the front vent after 0.12 s. The observation is consistent with the infrared images shown in Fig. 6.

At 0.14 s, a gas cloud (~2 m long and 1 m tall) appears outside the vent in the atmosphere with ~9% H_2 in the centre. The gas temperature is less than 600°C. The gas cloud is quickly blown away from the vent and the concentration also deceases quickly to below the flammable range (<4%). Combustion does not occur in the atmosphere in the simulation. Burnt gas (~1200°C in the centre) is continuously vented out from the front chamber and expands to about 6 m away from the vent at 0.20 s.

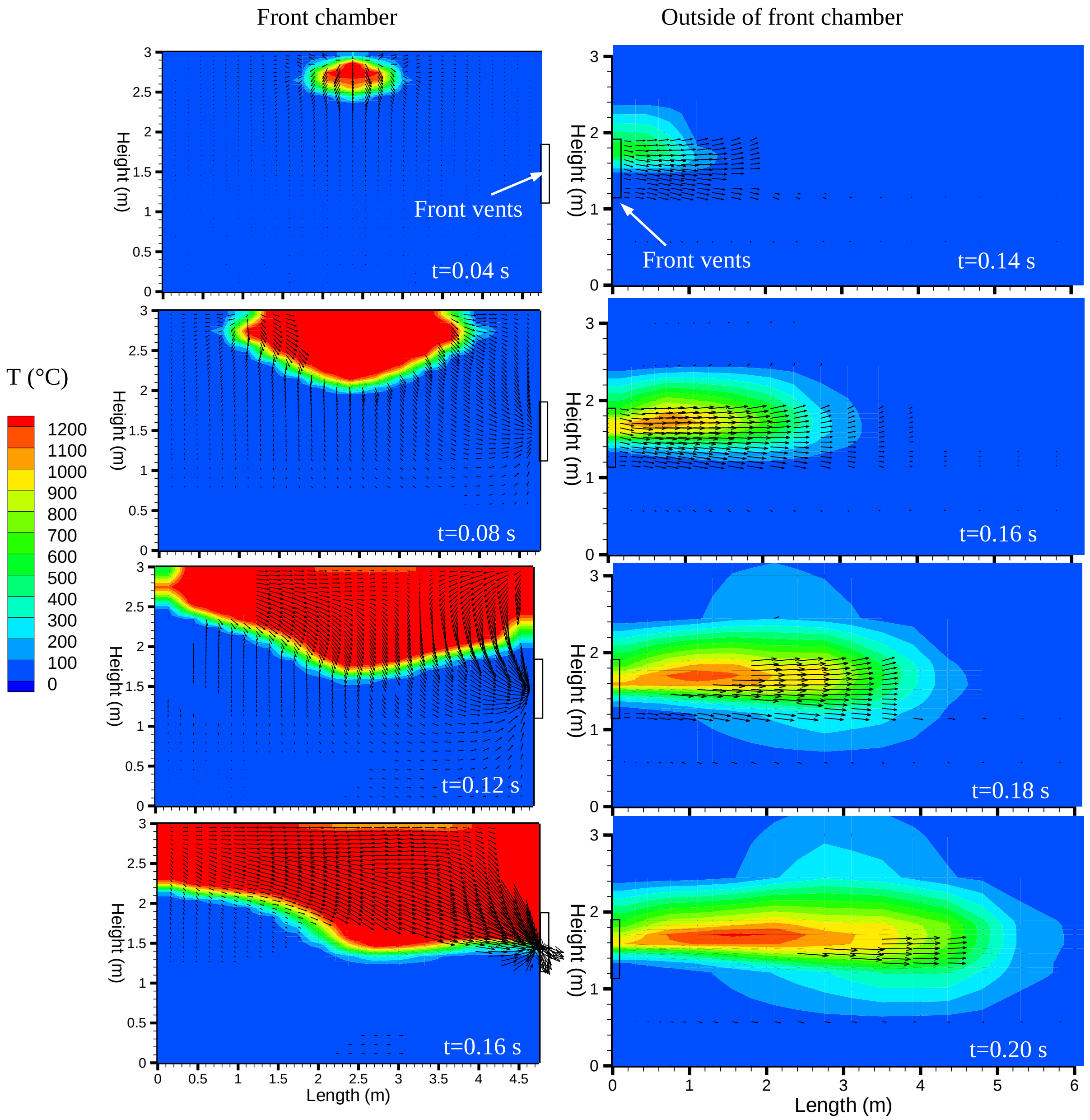

Figure 7. Contour plots of gas temperature inside (left column) and outside (right column) of front chamber predicted by GOTHIC for 24% H_2 (the maximum) with a -0.29%/cm gradient

4.3 Flame Speed

In Fig. 8, the flame front location is plotted as a function of the flame arrival time along the centre line between the igniter and the front or centre wall. The flame arrival time represents the instance when the gas temperature exceeds 40°C at each thermocouple location in the experiment and at each computational cell in the simulation across the ceiling between the front and centre wall.

As a result of the limited accuracy in determining the flame arrival time, an average flame propagation speed is calculated based on the linear distance-time profile. The average measured flame speed is around 19.5 m/s towards the vent and 18.4 m/s towards the centre wall. The GOTHIC prediction is slightly higher (close to 28.6 m/s towards the vent and 25.9 m/s towards the centre wall). The flame propagation speed is the same in both directions within a distance of 1 m from the igniter, but it becomes greater towards the vent after the vent rupture. The trend is consistent with the pressure transients shown in Fig. 5 and infrared images shown in Fig. 6. The time to reach the maximum overpressure shown in Fig. 5 is aligned with the time when the flame front passes the thermocouple at a distance of 1.75 m (close to the front wall), suggesting that the flame has reached its maximum surface area when it arrives at the front wall and, therefore, the acoustic effect has no further contribution to the combustion.

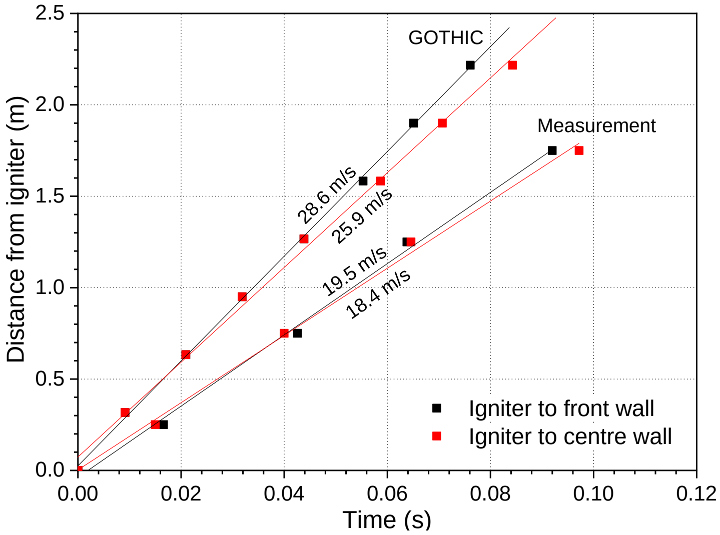

Figure 8. Comparison of average flame propagation speed at ceiling between measurement and GOTHIC simulation

4.4 Peak Overpressure

The measured peak overpressure as a function of the maximum hydrogen concentration is compared with the GOTHIC predictions in Fig. 9. The trending lines of the peak overpressure are an exponential fit to the measurements or predictions. The maximum overpressure increases exponentially with an increase in the maximum H_2 concentration in the layer. The GOTHIC predictions closely follow the trend of the measurements, but the peak overpressures are always over-predicted. The agreement is within a range of 50% (relative) or 6 kPa (absolute).

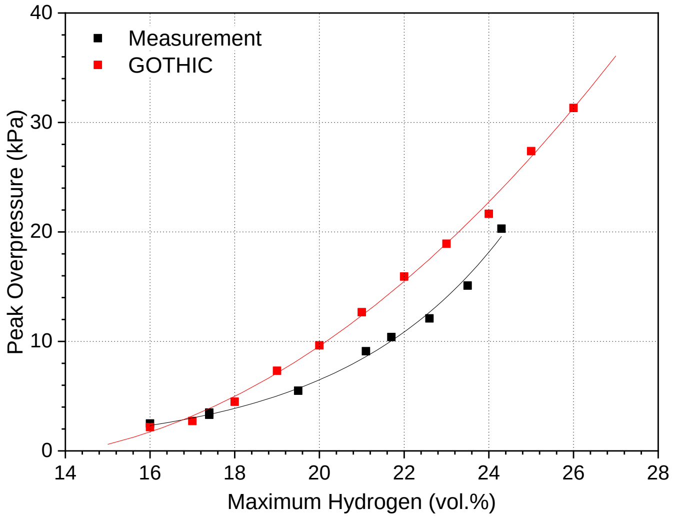

Figure 9. Comparison of peak overpressure as a function of maximum H_2 concentration between measurement and GOTHIC simulation

The measured peak overpressures are compared in Fig. 10 with a model prediction using the approach of Molkov and Bragin [12], assuming that the hydrogen is uniformly mixed within the stratified layer. The combustion properties of unburnt mixtures (namely, the burning velocity, sound speed, and expansion ratio) used in Molkov and Bragin's correlation [12] were based on the layer-averaged hydrogen concentration and the data were taken from the same reference. The venting parameter was defined using the volume occupied by the stratified hydrogen layer (upper region of the front chamber). A constant vent failure overpressure of 5 kPa was applied.

Liang [8] showed that the LSVCTF well-mixed combustion quiescent tests tend to be largely over-predicted by Molkov and Bragin's method [12], but the agreement is within a factor of 2 for turbulent tests. For the current study, the Molkov and Bragin predictions closely follow the trend of the measurements, as shown in Fig. 10. The good agreement suggests that the peak pressure of the stratified combustion tests may follow a trend similar to that of the well-mixed tests for a given layer-averaged hydrogen concentration; however, the total hydrogen mass in the well-mixed test is much higher than in the stratified test. In fact, as shown in Table 1, all the tests performed in the present study have volume-averaged hydrogen concentrations of less than 4% if well mixed in the front chamber, which would not be flammable.

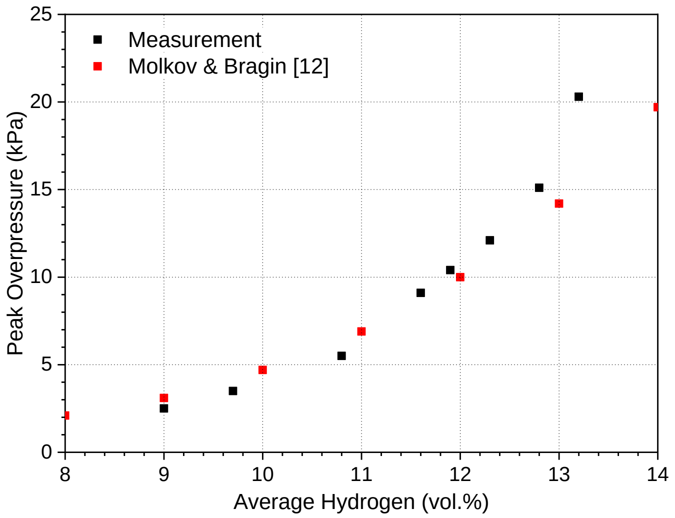

Figure 10. Comparison of measured peak overpressure as a function of average hydrogen concentration in layer with predictions using Molkov and Bragin's model [12]

5.0 CONCLUSIONS

The experiments performed in CNL's Large-Scale Vented Combustion Test Facility have shown that the combustion overpressure in stratified hydrogen layers increases exponentially with an increase in the maximum hydrogen concentration. The GOTHIC model predictions for the pressure dynamics of combustion in stratified layers are in relatively good agreement with the measurements, but the peak overpressures are over-predicted, especially with higher maximum hydrogen concentrations. Molkov and Bragin's predictions are consistent with the measured combustion peak overpressures based on the layer-averages hydrogen concentration, suggesting that the combustion behaviour in the present tests can be characterized by the average layer concentration, which depends on the maximum hydrogen and layer gradient. Although the combustion overpressure of the stratified tests is similar to that of the well-mixed tests for a given layer-averaged hydrogen concentration, the total hydrogen mass of the stratified tests is only ~20–25% that of the well-mixed tests. The risk of hydrogen combustion is more severe if the hydrogen is concentrated locally (for example by steam condensation) rather than well mixed in a volume; therefore, promoting mixing in a post-accident atmosphere to eliminate hydrogen accumulation is beneficial in reducing the hydrogen combustion risk.

ACKNOWLEDGEMENT

The authors gratefully acknowledges the financial support from the Canadian Nuclear Safety Commission and Atomic Energy of Canada Limited, under the auspices of the Federal Nuclear Science and Technology Program.

REFERENCE

1. Status Report on Hydrogen Management and Related Computer Codes, NEA/CSNI/R(2014)8, 2014.
2. Whitehouse, D.R., Greig, D.R., and Koroll, G.W., Combustion of Stratified Hydrogen-Air Mixtures in the 10.7 m^3 Combustion Test Facility Cylinder, *Nucl Eng Des*, **166**, 1996, pp. 453–462.
3. Bleyer, A., Taveau, J., Djebaïli-Chaumeix, N., Paillard, C.E., and Bentaïb, A., Comparison between FLACS Explosion Simulations and Experiments Conducted in a PWR Steam Generator Casemate Scale Down with Hydrogen Gradients, *Nucl Eng Des*, **245**, 2012, pp. 189–196.
4. Vollmer, K.G., Ettner, F., and Sattelmayer, T., Deflagration to Detonation Transition in Hydrogen/Air Mixtures with a Concentration Gradient, *Combust Sci Technol*, **184**, 2012, pp. 1903-1915.
5. Kuznetsov, M., Grune, J., Friedrich, A., Sempert, K., Breitung, W., and Jordan, T., Hydrogen–Air Deflagrations and Detonations in Semi-Confined Flat Layer, Proceedings of the 6th International Seminar on Fire & Explosion Hazards (FEH6), Leeds, United Kingdom, 2010 April 11-16.
6. Rudy, W., Kuznetsov, M., Porowski, R., Teodorczyk, A., Grune, J., and Sempert, K., Critical Conditions of Hydrogen–Air Detonation in Partially Confined Geometry, *Proc Combust Inst*, **34** (2), 2013, pp. 1965–1972.
7. Grune, J., Sempert, K., Haberstroh, H., Kuznetsov, M., and Jordan, T., Experimental Investigation of Hydrogen–Air Deflagrations and Detonations in Semi-Confined Flat Layers, *J Loss Prevent Proc*, **26** (2), 2013, pp. 317–323.
8. Liang, Z., Scaling Effects of Vented Deflagrations for Near Lean Flammability Limit Hydrogen-Air Mixtures in Large Scale Rectangular Volumes, *Int J Hydrog Energy*, **42** (10), 2017, pp. 7089-7103.
9. Liang, Z. Vented Deflagrations for Near Lean Flammability Limit Hydrogen-Air Mixtures in Large Scale Inter-Connected Volumes, *Int J Hydrog Energy*, **42** (20), 2017, pp. 14321–14331.
10. Carcassi, M.N. and Fineschi, F., Deflagrations of H_2–Air and CH_4–Air Lean Mixtures in a Vented Multi-Compartment Environment, *Energy*, **30** (8), 2005, pp. 1439–1451.
11. Chao, J., Bauwens, C.R., and Dorofeev, S.B., An Analysis of Peak Overpressures in Vented Gaseous Explosions, *Proc Combust Inst*, **33**, 2011, pp. 2367–2374.
12. Molkov, V.V. and Bragin, M., Hydrogen-Air Deflagrations: Vent Sizing Correlation for Low-Strength Equipment and Buildings", *Int J Hydrog Energy*, **40**(2), 2015, pp. 1256–1266.
13. Liang, Z., Gardner, L., Clouthier, T., and MacCoy, R., Hydrogen Deflagration in Stratified Flat Layers in Single or Interconnected Large Rectangular Volumes, Proceedings of the 12th International Topical Meeting on Nuclear Reactor Thermal-Hydraulics, Operation and Safety (NUTHOS-12), Qingdao, Shandong, China, 2018 October 14–18.
14. Voelsing, K., GOTHIC Thermal Hydraulic Analysis Package Technical Manual Version 8.2 (QA), Electric Power Research Institute Inc., 2016 October.
15. Cariteau, B. and Tkatschenko, I., Experimental Study of the Concentration Build-Up Regimes in an Enclosure without Ventilation, *Int J Hydrog Energy*, **37**, 2012, pp. 17400–17408.
16. Denisenko, V.P., Kirillov, I.A., Korobtsev, S.V., and Nikolaev, I.I., Hydrogen Distribution in Enclosures: on Distinction Criterion between Quasi-Homogeneous Mixing and Stratification Modes, Proceedings of 6th International Conference on Hydrogen Safety (ICHS), Brussels, Belgium, 2013 September 09–11.